

Chiral fluctuations in MnSi above the Curie temperature

B. Roessli¹, P. Böni², W. E. Fischer¹ and Y. Endoh³

¹Laboratory for Neutron Scattering, ETH Zurich & Paul Scherrer Institute, CH-5232 Villigen PSI

²Physik-Department E21, Technische Universität München, D-85747 Garching, Germany

³Physics Department, Tohoku University, Sendai 980, Japan

(February 1, 2008)

Polarized neutrons are used to determine the antisymmetric part of the magnetic susceptibility in non-centrosymmetric MnSi. The paramagnetic fluctuations are found to be incommensurate with the chemical lattice and to have a chiral character. We argue that antisymmetric interactions must be taken into account to properly describe the critical dynamics in MnSi above T_C . The possibility of directly measuring the polarization dependent part of the dynamical susceptibility in a large class of compounds through polarised inelastic neutron-scattering is outlined as it can yield direct evidence for antisymmetric interactions like spin-orbit coupling in metals as well as in insulators.

PACS numbers: 75.25+z, 71.70.Ej, 71.20.lp

Ordered states with helical arrangement of the magnetic moments are described by a chiral order parameter $\vec{C} = \vec{S}_1 \times \vec{S}_2$, which yields the left- or right-handed rotation of neighboring spins along the pitch of the helix. Examples for compounds of that sort are rare-earth metals like Ho [1]. Spins on a frustrated lattice form another class of systems, where simultaneous ordering of chiral and spin parameters can be found. For example, in the triangular lattice with antiferromagnetic nearest neighbor interaction, the classical ground-state is given by a non-collinear arrangement with the spin vectors forming a 120° structure. In this case, the ground state is highly degenerate as a continuous rotation of the spins in the hexagonal plane leaves the energy of the system unchanged. In addition, it is possible to obtain two equivalent ground states which differ only by the sense of rotation (left or right) of the magnetic moments from sub-lattice to sub-lattice, hence yielding an example of chiral degeneracy.

As a consequence of the chiral symmetry of the order parameter, a new universality class results that is characterized by novel critical exponents as calculated by Monte-Carlo simulations [2] and measured by neutron scattering [3] in the XY-antiferromagnet CsMnBr₃. An interesting but still unresolved problem is the characterization of chiral spin fluctuations that have been suggested to play an important role e.g. in the doped high- T_c superconductors [4]. The measurement of chiral fluctuations is, however, a difficult task and can usually only be performed by projecting the magnetic fluctuations on a field-induced magnetization [5,6].

In this Letter, we show that chiral fluctuations can be directly observed in non-centrosymmetric crystals without disturbing the sample by a magnetic field. We present results of polarized inelastic neutron scattering experiments performed in the paramagnetic phase of the itinerant ferromagnet MnSi that confirm the chiral char-

acter of the spin fluctuations due to spin-orbit coupling and discuss the experimental results in the framework of self-consistent renormalisation theory of spin-fluctuations in itinerant magnets [7].

Being a prototype of a weak itinerant ferromagnet, the magnetic fluctuations in MnSi have been investigated in the past in detail by means of unpolarized and polarized neutron scattering. The results demonstrate the itinerant nature of the spin fluctuations [8–10] as well as the occurrence of spiral correlations [11] and strong longitudinal fluctuations [13].

MnSi has a cubic space group $P2_13$ with a lattice constant $a = 4.558 \text{ \AA}$ that lacks a center of symmetry leading to a ferromagnetic spiral along the $[1\ 1\ 1]$ direction with a period of approximately 180 \AA [14]. The Curie temperature is $T_C = 29.5 \text{ K}$. The spontaneous magnetic moment of Mn $\mu_s \simeq 0.4\mu_B$ is strongly reduced from its free ion value $\mu_f = 2.5\mu_B$. As shown in the inset of Fig. 1 the four Mn and Si atoms are placed at the positions (x, x, x) , $(\frac{1}{2}+x, \frac{1}{2}-x, -x)$, $(\frac{1}{2}-x, -x, \frac{1}{2}+x)$, and $(-x, \frac{1}{2}+x, \frac{1}{2}-x)$ with $x_{Mn} = 0.138$ and $x_{Si} = 0.845$, respectively.

We investigated the paramagnetic fluctuations in a large single crystal of MnSi (mosaic $\eta = 1.5^\circ$) of about 10 cm^3 on the triple-axis spectrometer TASP at the neutron spallation source SINQ using a polarized neutron beam. The single crystal was mounted in a ^4He refrigerator of ILL-type and aligned with the $[0\ 0\ 1]$ and $[1\ 1\ 0]$ crystallographic directions in the scattering plane. Most constant energy-scans were performed around the $(0\ 1\ 1)$ Bragg peak and in the paramagnetic phase in order to relax the problem of depolarization of the neutron beam in the ordered phase. The spectrometer was operated in the constant final energy mode with a neutron wave vector $\vec{k}_f = 1.97 \text{ \AA}^{-1}$. In order to suppress contamination by higher order neutrons a pyrolytic graphite filter was installed in the scattered beam. The incident neutrons were polarized by means of a remanent [15] FeCoV/TiN-

type bender that was inserted after the monochromator [16]. The polarization of the neutron beam at the sample position was maintained by a guide field $B_g = 10$ G that defines also the polarization of the neutrons \vec{P}_i with respect to the scattering vector $\vec{Q} = \vec{k}_i - \vec{k}_f$ at the sample position.

In contrast to previous experiments, where the polarization \vec{P}_f of the scattered neutrons was also measured in order to distinguish between longitudinal and transverse fluctuations [13], we did not analyze \vec{P}_f , as our goal was to detect a polarization dependent scattering that is proportional to $\sigma_p \propto (\hat{\vec{Q}} \cdot \vec{P}_i)$ as discussed below.

A typical constant-energy scan with $\hbar\omega = 0.5$ meV measured in the paramagnetic phase at $T = 31$ K is shown in Fig. 1 for the polarization of the incident neutrons \vec{P}_i parallel and anti-parallel to the scattering vector \vec{Q} . It is clearly seen that the peak positions depend on \vec{P}_i and appear at the incommensurate positions $\vec{Q} = \vec{\tau} \pm \vec{\delta}$ with respect to the reciprocal lattice vector $\vec{\tau}_{011}$ of the nuclear unit cell. Obviously, this shift of the peaks with respect to (0 1 1) would be hardly visible with unpolarized neutrons and could not be observed in previous inelastic neutron works.

In order to discuss our results we start with the general expression for the cross-section of magnetic scattering with polarized neutrons [12]

$$\begin{aligned} \frac{d^2\sigma}{d\Omega d\omega} \sim & \sum_{\alpha,\beta} (\delta_{\alpha,\beta} - \hat{Q}_\alpha \hat{Q}_\beta) A^{\alpha\beta}(\vec{Q}, \omega) \\ & + \sum_{\alpha,\beta} (\hat{\vec{Q}} \cdot \vec{P}_i) \sum_{\gamma} \epsilon_{\alpha,\beta,\gamma} \hat{Q}_\gamma B^{\alpha\beta}(\vec{Q}, \omega) \end{aligned} \quad (1)$$

where (\vec{Q}, ω) are the momentum and energy-transfers from the neutron to the sample, $\hat{\vec{Q}} = \vec{Q}/|\vec{Q}|$, and α, β, γ indicate Cartesian coordinates. The first term in Eq. 1 is independent of the polarization of the incident neutrons, while the second is polarization dependent through the factor $(\hat{\vec{Q}} \cdot \vec{P}_i)$. \vec{P}_i denotes the direction of the neutron polarization and its scalar is equal to 1 when the beam is fully polarized. $A^{\alpha\beta}$ and $B^{\alpha\beta}$ are the symmetric and antisymmetric parts of the scattering function $S^{\alpha\beta}$, that is $A^{\alpha\beta} = \frac{1}{2}(S^{\alpha\beta} + S^{\beta\alpha})$ and $B^{\alpha\beta} = \frac{1}{2}(S^{\alpha\beta} - S^{\beta\alpha})$. $S^{\alpha\beta}$ are the Fourier transforms of the spin correlation function $\langle s_l^\alpha s_{l'}^\beta \rangle$, $S^{\alpha\beta}(\vec{Q}, \omega) = \frac{1}{2\pi N} \int_{-\infty}^{\infty} dt e^{-i\omega t} \sum_{ll'} e^{i\vec{Q}(\vec{X}_l - \vec{X}_{l'})} \langle s_l^\alpha s_{l'}^\beta(t) \rangle$. The vectors \vec{X}_l designate the positions of the scattering centers in the lattice. The correlation function is related to the dynamical susceptibility through the fluctuation-dissipation theorem $S(\vec{Q}, \omega) = 2\hbar/(1 - \exp(-\hbar\omega/kT))\Im\chi(\vec{Q}, \omega)$.

Following Ref. [17] we define now an axial vector \vec{B} by $\sum_{\alpha,\beta} \epsilon_{\alpha\beta\gamma} B^{\alpha\beta} = B^\gamma(\vec{Q}, \omega)$, that represents the antisymmetric part of the susceptibility which, hence, depends on the neutron polarization as follows

$$(\hat{\vec{Q}} \cdot \vec{P}_i)(\hat{\vec{Q}} \cdot \vec{B}) \quad (2)$$

and vanishes for centro-symmetric systems or when there is no long-range order. In the absence of symmetry breaking fields like external magnetic fields, pressure etc., similar scans with polarized neutrons would yield a peak of diffuse scattering at the zone center and no scattering that depends on the polarization of the neutrons. However, an intrinsic anisotropy of the spin Hamiltonian in a system that lacks lattice inversion symmetry may provide an axial interaction leading to a polarization dependent cross section. The polarization dependent scattering obtained in the present experiments is therefore an indication of fluctuations in the chiral order parameter and points towards the existence of an axial vector \vec{B} that is not necessarily commensurate with the lattice. Hence, according to Eq. 2 the neutron scattering function in MnSi contains a non-vanishing antisymmetric part.

Because the crystal structure of MnSi is non-centrosymmetric and the magnetic ground-state forms a helix with spins perpendicular to the [1 1 1] crystallographic direction, it is reasonable to interpret the polarization-dependent transverse part of the dynamical susceptibility in terms of the Dzyaloshinskii-Moriya (DM) interaction [20,21] similarly as it was done in other non-centrosymmetric systems that show incommensurate ordering [18,19].

Usually the DM-interaction is written as the cross product of interacting spins $H_{DM} = \sum_{l,m} \vec{D}_{l,m} \cdot (\vec{s}_l \times \vec{s}_m)$, where the direction of the DM-vector \vec{D} is determined by bond symmetry and its scalar by the strength of the spin-orbit coupling [21]. Although the DM-interaction was originally introduced on microscopic grounds for ionic crystals, it was shown that antisymmetric spin interactions are also present in metals with non-centrosymmetric crystal symmetry [22]. In a similar way as for insulators with localized spin densities, the antisymmetric interaction originates from the spin-orbit coupling in the absence of an inversion center and a finite contribution to the antisymmetric part of the wave-vector dependent dynamical susceptibility is obtained.

For the case of a uniform DM-interaction, the neutron cross-section depends on the polarization of the neutron beam [23] as follows

$$\begin{aligned} \left(\frac{d^2\sigma}{d\Omega d\omega} \right)_{np} & \sim \Im(\chi^\perp(\vec{q} - \vec{\delta}, \omega) + \chi^\perp(\vec{q} + \vec{\delta}, \omega)), \\ \left(\frac{d^2\sigma}{d\Omega d\omega} \right)_p & \sim (\hat{\vec{D}} \cdot \hat{\vec{Q}})(\hat{\vec{Q}} \cdot \vec{P}_i) \\ & \times \Im(\chi^\perp(\vec{q} - \vec{\delta}, \omega) - \chi^\perp(\vec{q} + \vec{\delta}, \omega)). \end{aligned} \quad (3)$$

Here, \vec{q} designates the reduced momentum transfer with respect to the nearest magnetic Bragg peak at $\vec{\tau} \pm \vec{\delta}$. The first line of Eq. 3 describes inelastic scattering with a non-polarized neutron beam. The second part describes

inelastic scattering that depends on \vec{P}_i as well as on \vec{Q} . Eq. 3 shows that the cross section for $\vec{P}_i \perp \vec{Q}$ is indeed independent of P_i as observed in Fig. 2. By subtracting the inelastic spectra taken with \vec{P}_i parallel and anti-parallel to \vec{Q} , the polarization dependent part of the cross-section can be isolated, as demonstrated in Fig. 3 for two temperatures $T = 31$ K and $T = 40$ K.

Close to T_C , the intensity is rather high and the crossing at $Q = (0\ 1\ 1)$ is sharp. At 40 K the intensity becomes small and the transition at $(0\ 1\ 1)$ is rather smooth, which mirrors the decreases of the correlation length with increasing temperature. We have measured $(d^2\sigma/(d\Omega d\omega))_p$ in the vicinity of the $(0\ 1\ 1)$ Bragg peak at $T = 35$ K. The result shown as a contour plot in Fig. 4 indicates that the DM-interaction vector in MnSi has a component along the $[0\ 1\ 1]$ crystallographic direction which induces paramagnetic fluctuations centered at positions incommensurate with the chemical lattice.

In order to proceed further with the analysis we assume for the transverse susceptibilities in Eq. 3 the expression for itinerant magnets as given by self-consistent re-normalization theory (SCR) [7]

$$\chi^\perp(\vec{q} \pm \vec{\delta}, \omega) = \chi^\perp(\vec{q} \pm \vec{\delta}) / (1 - i\omega / \Gamma_{\vec{q} \pm \vec{\delta}}). \quad (4)$$

$\vec{\delta}$ is the ordering wave-vector, $\chi^\perp(\vec{q} \pm \vec{\delta}) = \chi^\perp(\vec{q}) / (1 + q^2 / \kappa_\delta^2)$ the static susceptibility, and κ_δ the inverse correlation length. For itinerant ferromagnets the damping of the spin fluctuations is given by $\Gamma_{\vec{q} \pm \vec{\delta}} = uq(q^2 + \kappa_\delta^2)$ with $u = u(\vec{\delta})$ reflecting the damping of the spin fluctuations. Experimentally, it has been found from previous inelastic neutron scattering measurements that the damping of the low-energy fluctuations in MnSi is adequately described using the results of the SCR-theory rather than the q^z ($z = 2.5$) wave-vector dependence expected for a Heisenberg magnet [9].

The solid lines of Figs. 1 to 3 show fits of $(d^2\sigma/(d\Omega d\omega))_p$ to the polarized beam data. It is seen that the cross section for itinerant magnets reproduces the data well if the incommensurability is properly taken into account. Using Eqs. 3 and 4 and taking into account the resolution function of the spectrometer, we extract values $\kappa_0 = 0.12\ \text{\AA}^{-1}$ and $u = 27\ \text{meV}\text{\AA}^3$ in reasonable agreement with the analysis given in Ref. [10]. The smaller value for u when compared with $u = 50\ \text{meV}\text{\AA}^3$ from Ref. [9] indicates that the incommensurability $\vec{\delta} = (0.02, 0.02, 0.02)$ was neglected in the analysis of the non-polarized neutron data. At $T = 40$ K, the chiral fluctuations are broad (Fig. 3) due to the increase of κ_δ with increasing T , i.e. $\kappa_\delta(T) = \kappa_0(1 - T_C/T)^\nu$. We note that the mean-field-like value $\nu = 0.5$ obtained here is close to the expected exponent $\nu = 0.53$ for chiral symmetry [2]. This suggests that a chiral-ordering transition also occurs in MnSi in a similar way to the rare-earth compound Ho, pointing toward the existence of a universality class in the magnetic ordering of helimagnets [1].

In conclusion, we have shown that chiral fluctuations can be measured by means of polarized inelastic neutron scattering in zero field, when the antisymmetric part of the dynamical susceptibility has a finite value. We have shown that this is the case in metallic MnSi that has a non-centrosymmetric crystal symmetry. For this compound the axial interaction leading to the polarized part of the neutron cross-section has been identified as originating from the DM-interaction. Similar investigations can be performed in a large class of other physical systems. They will yield direct evidence for the presence of antisymmetric interactions in forming the magnetic ground-state in magnetic insulators with DM-interactions, high- T_c superconductors (e.g. La_2CuO_4 [24]), nickelates [25], quasi-one dimensional antiferromagnets [26] or metallic compounds like FeGe [27].

-
- [1] V.P. Plakhty et al., Phys. Rev. B **64**, 100402(R), 2001.
 - [2] H. Kawamura, Phys. Rev. B **38** 4916 (1988).
 - [3] T.E. Mason et al., Phys. Rev. B **39** 586 (1989).
 - [4] P.E. Sulewski et al., Phys. Rev. Lett. **67**, 3864 (1991).
 - [5] S. V. Maleyev, Phys. Rev. Lett. **75**, 4682 (1995).
 - [6] V. P. Plakhty et al., Europhys. Lett. **48**, 215 (1999).
 - [7] T. Moriya, in *Spin Fluctuations in Itinerant Electron Magnetism* **56**, Springer-Verlag, Berlin Heidelberg New-York Tokyo, 1985.
 - [8] Y. Ishikawa et al., Phys. Rev. B **16**, 4956 (1977).
 - [9] Y. Ishikawa et al., Phys. Rev. B **25**, 254 (1982).
 - [10] Y. Ishikawa et al., Phys. Rev. B **31**, 5884 (1985).
 - [11] G. Shirane et al., Phys. Rev. B **28**, 6251 (1983).
 - [12] e.g. Yu A. Izyumov, Sov. Phys. Usp. **27**, 845 (1984).
 - [13] S. Tixier et al., Physica B **241-243**, 613, (1998).
 - [14] Y. Ishikawa et al., Solid. State. Commun. **19**, 525 (1976).
 - [15] No spin flipping devices are necessary due to the remanent magnetization of the supermirror coatings of the benders. For details see: P. Böni et al., Physica B **267-268**, (1999) 320.
 - [16] F. Semadeni, B. Roessli, and P. Böni, Physica B **297**, 152 (2001).
 - [17] S.W. Lovesey and E. Balcar, Physica B **267-268**, 221 (1999).
 - [18] A. Zheludev et al., Phys. Rev. Lett. **78**, (1997) 4857.
 - [19] B. Roessli et al., Phys. Rev. Lett. **86** (2001) 1885.
 - [20] L. Dzyaloshinskii, J. Phys. Chem. Solids **4**, 241 (1958).
 - [21] T. Moriya, Phys. Rev. **120**, 91 (1960).
 - [22] M. Kataoka et al., J. Phys. Soc. Japan **53**, 3624 (1984).
 - [23] D.N. Aristov and S.V. Maleyev Phys. Rev. B **62** (2000) R751.
 - [24] J. Berger and A. Aharony, Phys. Rev. B **46**, 6477 (1992).
 - [25] W. Koshibae, Y. Ohta and S. Maekawa, Phys. Rev. B **50**, 3767 (1994).
 - [26] I. Tsukada et al., Phys. Rev. Lett. **87**, 127203 (2001).
 - [27] B. Lebech, J. Bernhard, and T. Freltoft, J. Phys.: Condens. Matter **1**, 6105 (1989).

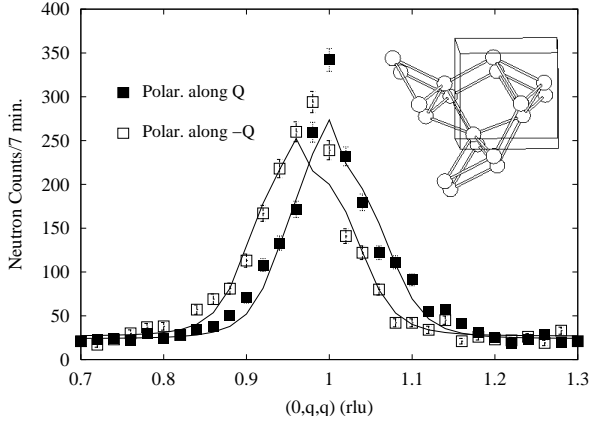


FIG. 1. Inelastic spectra in MnSi ($\hbar\omega = 0.5$ meV) at $T = 31$ K for the neutron polarization parallel and anti-parallel to the scattering vector \vec{Q} , respectively. The solid lines are fits to the data. The inset shows the Mn atoms in the crystal structure of MnSi. Note that MnSi is not centro-symmetric.

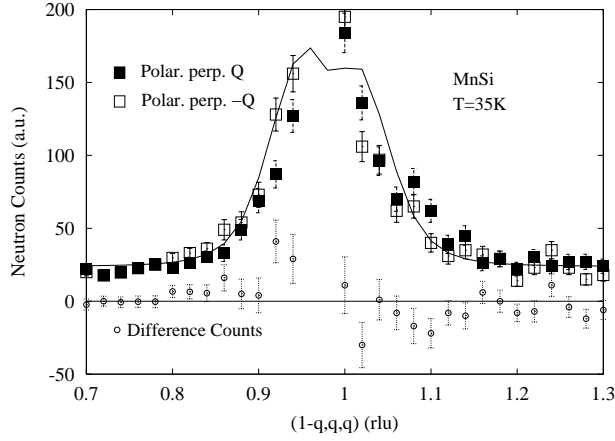


FIG. 2. Neutron spectra in MnSi for an energy-transfer $\hbar\omega = 0.5$ meV as measured at $T = 35$ K for \vec{P}_i perpendicular to \vec{Q} and $-\vec{Q}$, respectively. The solid line shows a fit to the data and the small symbols represent the difference signal that is independent of \vec{P}_i . See text for details.

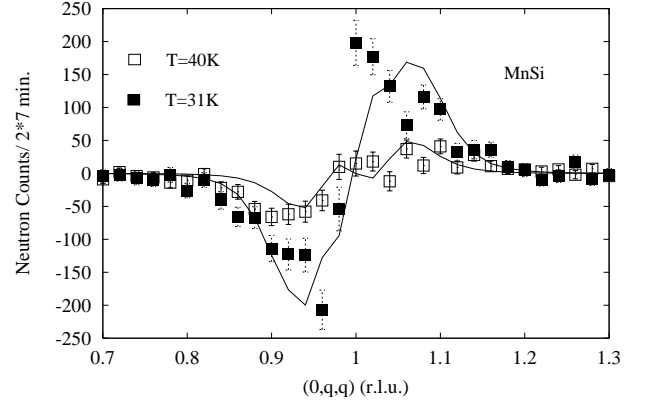


FIG. 3. Difference neutron counts for polarization \vec{P}_i of the incident neutron beam parallel and anti-parallel to \vec{Q} in MnSi at $T = 31$ K and 40 K, respectively. The solid lines are fit to the data using the SRC-result for the dynamical susceptibility with the parameters given in the text.

FIG. 4. Contour-map of the polarization dependent scattering for an energy transfer $\hbar\omega = 0.5$ meV as measured near the (0 1 1) reciprocal lattice point at $T=35$ K.

MnSi, Observed Chiral Fluctuations

